RSC Advances

PAPER

View Article Online
View Journal | View Issue

Cite this: *RSC Adv.*, 2014, **4**, 40146

Uniform silica coating of isoprene-passivated germanium nanowires *via* Stöber method

Shu-Hao Chang, Yu-Tung Tsai, Guo-An Li, Shao-Lou Jheng, Tzu-Lun Kao and Hsing-Yu Tuan*

Received 22nd May 2014
Accepted 26th August 2014

DOI: 10.1039/c4ra04858j

www.rsc.org/advances

Encapsulation of an amorphous silica shell can significantly enhance the thermal and chemical stability of core materials. Traditional silica coating methods on semiconductors such as silicon (Si) and germanium (Ge) mostly involve various high-temperature oxidation processes. This paper describes a solution-based Stöber method for the coating of Ge nanowires (NWs) with a uniform shell of amorphous silica. Ge–silica core–shell NWs were prepared by mixing isoprene-protected Ge NWs with tetraethyl orthosilicate (TEOS) and ammonia solution. The SiO_2 species migrated around the surface of the Ge NWs and were incorporated onto the nanowire through hydrolysis and condensation of TEOS in ammonia solution. Without isoprene passivation, Ge NWs easily oxidize upon exposure to ambient conditions to form a GeO_{2-x} shell, which renders them water-soluble and makes the NWs inapplicable. We also show that the thickness of the silica shell can be tuned with different reaction times. Finally, fluorescein isothiocyanate (FITC) incorporated on the Ge–silica core–shell structure was demonstrated.

Introduction

Germanium (Ge) is a candidate material for semiconductor devices that has lower resistivity and higher charge carrier mobility than silicon (Si).[1,2] One dimensional Ge has attracted much attention because of its important properties for numerous applications such as field-effect transistors (FETs) and lithium ion batteries.[3] Synthetic routes to produce Ge NWs include solvothermal, laser ablation, metal-seeded vapor–liquid–solid (VLS), supercritical-fluid–liquid–solid (SFLS) and solution–liquid–solid (SLS).[4–7] Typically, the yield of Ge NWs in SFLS growth is higher than that of Ge NWs prepared by conventional methods (60–80% for SFLS growth and 20–30% for VLS growth).[7] In addition, the liquid organometallic precursor (diphenylgermane, DPG, in our case) is safer and less harmful in comparison with gaseous precursor used for VLS growth. Ge surface easily forms the low quality water-soluble germanium oxide (GeO_{2-x}).[8] Slight surface oxidation significantly degrades nanowire performance in the case of electronic nanowire devices. As a result, silicon turns out to become the main stream material in semiconductor manufacturing instead of Ge.

Recently, many studies have been reported on the surface passivation of nanomaterials. Organic passivation of nanowires raises many beneficial properties such as better oxidation resistance, enhanced corrosion resistance, and improved dispersibility.[9] A variety of organic ligands, such as alkylthios,[10] aromatic thiols[11] and alkylamines,[12] have also achieved the passivation function in nanomaterial-based applications.[13] Several reports have also shown that with organic passivation, the semiconductor NWs field effect transistor (FET) performance wouldn't be influenced by water or gas molecules in ambient atmosphere,[14] and possibly further improve the performance.[15] Korgel *et al.* reported that Ge NWs passivated by an organic layer exhibited two orders of magnitude slower current relaxation and a smaller decrease in current compared to non-passivated one with oxidized surfaces.[16,17]

Silica is considered as a protective layer which mainly lies in its anomalously high stability in the wide range of solvent from polar to apolar, especially in aqueous media. Furthermore, functionalized silica is an excellent host material for fluorescent organic dyes which suited for applications in the sensor, biology and beyond.[18,19] Traditional silica coating process is carried out by carbothermal reduction of SiO_2 nanomaterials with active carbon at temperatures higher than 1250 °C in flowing nitrogen atmosphere.[20–25] Afzaal *et al.* provided a route to prepare PbS/SiO_2 coaxial structure by chemical vapor deposition (CVD) method on silicon substrate at temperature between 650 and 700 °C.[26] Zhang *et al.*[27] and Shi *et al.*[28] have employed a laser ablation method to synthesize the coaxial nanostructure containing a silica inter-layer and carbon outer-shell. For fabricating Ge–SiO_2 core–shell nanostructure, Huang *et al.* reported a conventional furnace system to prepare Ge–SiO_2 nanotubes.[29] Ge–SiO_2 nanocables have been fabricated by complicated two-step process which combined thermal evaporation of SiO powders and laser ablation of a Ge target.[30]

Department of Chemical Engineering, National Tsing Hua University, 101, Section 2, Kuang-Fu Road, Hsinchu, Taiwan 30013, ROC. E-mail: hytuan@che.nthu.edu.tw; Fax: +886-3-571-5408; Tel: +886-3-572-3661

Numerous studies have been conducted on silica coating of colloidal nanocrystals by aqueous methods. Stöber method is a common method to coat nanomaterials with silica shell. In 1968, Stöber *et al.* presented a water–alcohol–ammonia–tetraalkoxysilane system to prepare uniform size spherical silica particles by means of hydrolysis of alkyl silicates in alcoholic solutions.[31] In a typical process, hydrolysis and condensation of tetraethyl orthosilicate (TEOS) are performed in an ethanol–ammonia mixture, in which the homogeneous silica shells of variable thickness were coated onto the core material.[32,33] The Stöber method has been used to encapsulate quantum dots, polymer, metal and semiconductor nanomaterials, and metal oxide nanoparticles with silica layers.[34–43] In the past decade, the Stöber method was applied to more one-dimensional nanostructure, such as gold nanorods and nanowires.[44,45] However, to the best of our knowledge, the Stöber method has not applied to coat Ge NWs with silica.

Here, we develop an easier method to prepare Ge–silica coaxial nanowires with well-controlled shell thickness by the Stöber method. The procedure of silica coating involves the stability of core materials and chemical affinity to core materials and silica,[36] so the chemical surface modification process is necessary. The silica coating was carried out by reacting isoprene-passivated Ge NWs in the presence of ammonia solution, TEOS, cyclohexane and polyoxyethylene (5)-nonylphenyl ether (Igepal CO-520). In the reaction, ammonia served as a catalyst and Igepal CO-520 had proven as a good surfactant to control the size of the droplets in the silica coating procedure.[18] W/O microemulsions (water droplets dispersed in bulk oil) mechanism was used to explain the silica coating process. The isoprene passivated Ge NWs were transferred into W/O microemulsions prepared by mixing cyclohexane, ammonia solution and surfactant. At the same time, the hydrolysis and condensation of TEOS take place and form a uniform silica layer.[18,46] Precise control of the silica thickness with nanometer precision was achieved by tuning the length of reaction time. Furthermore, the Ge–silica core shell can serve as vehicles for introducing the organic dyes as fluorescent imaging agents. 3-aminopropyltriethoxysilane (APTES) was used to functionalize the silica shell followed by the fluorescein isothiocyanate (FITC) dye coating. The FITC-coated Ge–SiO_2 composite nanowires were investigated by fluorescence microscope.

Experimental section

Chemicals

All reagents were used as received. Diphenylgermane (DPG, $C_{12}H_{10}Ge$, 95%) was from Geleste. Isoprene ($CH_2{=}CHC(CH_3){=}CH_2$, ≧99%), hexane (C_6H_{14}, anhydrous, 95%), ethanol (C_2H_5OH, ≧99.8%), polyoxyethylene (5)-nonylphenyl ether (Igepal CO-520, $(C_2H_4O)_n{\cdot}C_{15}H_{24}O$, $n \sim 5$, average M_n: 441), cyclohexane (C_6H_{12}, ≧99%), ammonium hydroxide solution (NH_4OH solution, ACS reagent), tetraethyl orthosilicate (TEOS, $Si(OC_2H_5)_4$, 98%), (3-aminopropyl)triethoxysilane (APTES, $H_2N(CH_2)_3Si(OC_2H_5)_3$, ≧98%), fluorescein isothiocyanate (FITC, $C_{21}H_{11}NO_5S$, ≧90%) were from Sigma-Aldrich.

Synthesis of Ge nanowires

Ge NWs were synthesized *via* a slightly modified recipe of our previous work by the supercritical SFLS approach.[9] In the beginning, the titanium reactor was heated to 420 °C and increased the pressure to 600 psi by flushing hexane into the reactor. The 10 mL reactant solution was prepared by mixing diphenylgermane (DPG) with anhydrous hexane in the concentration of 500 mM followed by addition of dodecanethiol-coated Au nanocrystals. The Au : Ge mole ratio is 1 : 500 in this reaction. The Ge precursor was loaded into the injection loop and fed into the reactor at a flow rate of 0.5 mL min^{-1} to 1000 psi for 30 min. Before removing the NWs from the reactor, the Ge NWs were passivated with a monolayer of isoprene. The reactor was then cooled to 220 °C and was flushed with excess anhydrous supercritical hexane to remove by-products and unreacted reactants. The pressure was maintained at 500 psi and 10 mL of isoprene–hexane mixture with the volume ratio of 1 : 4 were added at a flow rate of 4 mL min^{-1} to 2500 psi and then reacted for 2 h. After the reaction, the reactor was cooled to room temperature and the Ge NWs were removed from the reactor. The nanowire product was purified by centrifugation with 30 mL of hexane–ethanol mixture with the volume ratio of 1 : 2 for three times.

Synthesis of core–shell Ge–SiO_2 NWs

5 mL of Igepal CO-520 was added to 85 mL of cyclohexane in a 250 mL Erlenmeyer flask and stirred at room temperature for 3 min. 5 mL of cyclohexane dispersion of Ge NWs (0.2 mg mL^{-1}) was added to the 85 mL cyclohexane solution and stirred for 5 min. 650 μL of aqueous NH_4OH solution (30% by volume) was added dropwise to the NWs dispersion, followed by the dropwise addition of 10 μL of TEOS. The mixture was sonicated for 30 min and stirred for 6, 12 and 18 h. The SiO_2-coated NWs were then purified by centrifuging for 10 min at 12000 rpm and the supernatant was discarded. The silica-coated NWs were stored as a concentrated dispersion for further characterization in ethanol.

Synthesis and functionalization of Ge–silica core–shell coaxial NWs by FITC dye

40 μL of 3-aminopropyltriethoxysilane (APTES) was added to the Ge–silica dispersed in 10 mL anhydrous ethanol, followed by the addition of 1 mL of ammonia. The resulting solution was stirred in the dark for 14 h. The product was centrifuged to remove the excess APTES and further washed with ethanol for three times, and dissolved in 10 mL ethanol. After wash, 10 mg of FITC was added to the Ge–silica–APTES NWs ethanol solution. This solution was stirred with the NWs at room temperature for 24 h in the dark. Finally, the product was collected using centrifugation at 8000 rpm for 10 min and the supernatant was discarded.

Characterization

The products were characterized by scanning electron microscopy (SEM), transmission electron microscopy (TEM), energy dispersive X-ray spectroscopy (EDS), X-ray diffraction (XRD),

attenuated total reflectance Fourier transform infrared (ATR-FTIR). SEM images were obtained using a HITACHI-S4700 field-emission SEM, operated with 5–15 kV accelerating voltage with working distances ranging between 10 to 20 mm. For TEM imaging, the nanowires dispersed in anhydrous ethanol were drop-cast onto a 200 mesh lacey carbon-coated copper grid (Electron Microscope Sciences). HRTEM and EDS were performed on a JEOL, JEM 2100F using 200 accelerating voltage equipped with an Oxford INCA EDX. XRD patterns were recorded by a Rigaku, Ultima IV X-ray diffractometer using Cu-Kα radiation source ($\lambda = 1.54$ Å) operated at 40 kV and 20 mA. UV-Vis absorption spectra were obtained using a Hitachi U-4100 spectrophotometer with the nanowires dispersed in DI water and photoluminescence (PL) spectra were taken using a Spex Fluorolog-3 Spectrophotometer.

Results and discussion

The schematic of experimental design for the growth of the core–shell nanowires is illustrated in Scheme 1.

The Ge NWs were prepared by decomposing DPG in the presence of Au nanocrystals in hexane at 420 °C and 1000 psi through SFLS method. From SEM images (Fig. 1), the diameter of Ge NWs is in the range of 40–60 nm, and the length is 20–60 μm, respectively. The chemical surface modification process was carried out by adding isoprene into the reaction. The isoprene-passivated Ge NWs showed more chemical stability than the untreated one.[16] In order to confirm the passivation condition on the Ge surface, FTIR measurement was applied to detect the functional group (Fig. 2). For disordered liquid-like alkane chains, the symmetric and asymmetric CH_2 stretches occur at 2855 and 2924 cm^{-1}. Isoprene chains with ordered packing lead to signals at lower vibrational frequency.[17] Without the isoprene passivation, there is no obvious peak in this range.

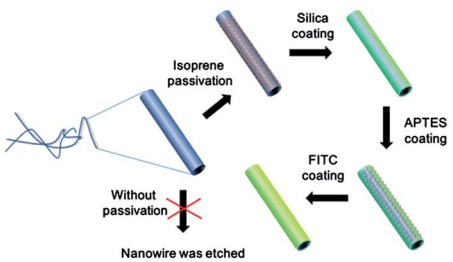

Scheme 1 Schematic illustration for the fabrication of Ge–silica core–shell structure and the decoration FITC.

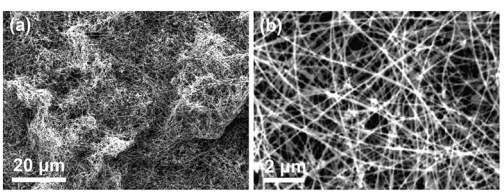

Fig. 1 SEM image of high-quality Ge NWs prepared by the SFLS method.

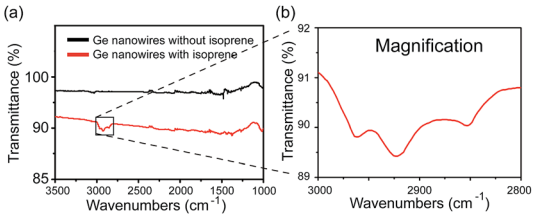

Fig. 2 The FTIR spectra of Ge NWs without isoprene (black line) and with isoprene (red line) modification.

Isoprene as a good passivation reagent for Ge NW has been proven before.[47,48] This passivation layer enhances the carrier mobility and prevent oxidation of Ge surface.[16] It is found that hydrolyzed TEOS has a high affinity for the Ge NW surface and easily form the silica layer onto it. Without the help of the isoprene layer, Ge NWs were oxidized and etched during the TEOS hydrolysis reaction.

Coating of these Ge NWs with amorphous silica was achieved using the Stöber method.[31] Ammonia is the widely-used catalyst for silica formation.[49] This process has been extensively exploited to form uniform coatings on nanoparticles since the growth occurs on a molecular scale.[32] Li *et al.* noted that the ammonia-catalyzed process follows the LaMer model in which accumulation of monomer reach the critical concentration for nucleation with a swift burst of nuclei and followed by the uniform shell growth without further nucleation.[41,50]

Further, the Ge NWs can indeed be transferred into water phase with the silica coating. The silica coated Ge NWs much improve the stability in DI water. Fig. 3a shows the results of the isoprene passivated Ge NWs dispersed in hexane (left), Ge NWs dispersed in DI water (middle) and Ge–silica core–shell NWs dispersed in DI water (right). The isoprene passivated Ge NWs can't be dispersed in DI water due to the hydrophobic property, which limit the applications in many fields. The Ge–silica core–shell NWs can be well-dispersed in DI water for more than 30 min, however, the isoprene passivated Ge NWs can't be well dispersed in hexane for a long time.

We also tried to apply the process directly on the bare Ge NWs without surface passivation. However, there appears serious surface etching compared to the one with isoprene passivation. The TEM images illustrated in Fig. 4 reveal the general morphology

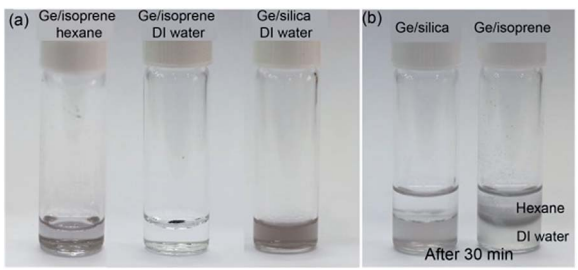

Fig. 3 (a) The photograph of Ge–isoprene NWs dispersed in hexane (left), Ge–isoprene NWs dispersed in DI water (middle), and Ge–silica core–shell nanowires dispersed in DI water. (b) The photograph of Ge–silica core–shell nanowires (left) and Ge–isoprene NWs (right) dispersed in the DI water and hexane mixture and stand for 30 min.

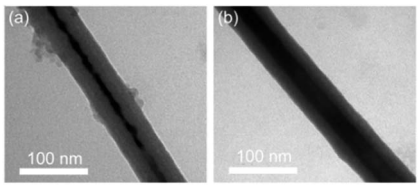

Fig. 4 TEM image of the Ge–silica core–shell NWs. (a) Ge NWs were not passivated with isoprene before the silica coating procedure. After silica coating, the Ge NWs were etched. (b) Ge NWs were passivated with isoprene before the silica coating procedure. After silica coating, Ge NWs were coated with a uniform layer of silica.

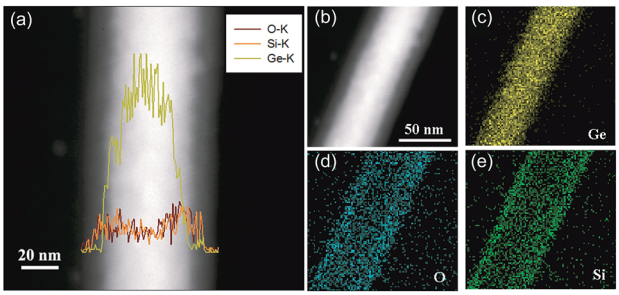

Fig. 6 Ge–silica core–shell structure line scan and EDS-mapping.

of the Ge–SiO_2 core–shell NWs with and without surface passivation. Without isoprene passivation, a layer of GeO_{2-x} formed and the nanowires were etched during reactions, resulting in non-smooth interface.

Fig. 5a shows typical SEM image of the silica-coated Ge NWs prepared using the Stöber method. The result demonstrated that the silica can be coated onto the isoprene-passivated Ge nanowire with high stability. Silica could be coated onto the surface of Ge NWs, however, by-products in the form of aggregated silica were also present in the sample. The XRD patterns of the as-prepared Ge NWs and Ge–SiO_2 core–shell NWs are shown in Fig. 5b. The amorphous nature of the silica layer was shown by the absence of XRD pattern, and no impurity peaks could be observed. From the TEM image, the product was primarily composed of Ge NWs with a uniform silica shell with diameter of 7.5 nm. High-resolution TEM (Fig. 5d) shows both single-crystal Ge NWs and amorphous silica shell with the interplanar spacing of 0.33 nm, corresponding to <111> growth direction.

To further verify the core–shell structure, STEM-EDS line scan and mapping were carried out. The line scan spectra in Fig. 6a shows clear germanium, silicon and oxygen signals. From the spectra, we can speculate that silicon is uniformly coated on the Ge surface. STEM-EDS mapping of core–shell NWs also confirms that Si and O are equally distributed around Ge NWs.

It has been proven that the thickness of silica layer could be controlled by changing the parameters (*e.g.* the concentration of the precursor solution and/or the reaction time).[51] We illustrated that this procedure can be extended to coat Ge NWs with controllable silica shell thickness. The shell thickness was directly proportional to the reaction time. We were able to vary the shell thickness in the range of 5–20 nm. Fig. 7 shows the TEM images of Ge NWs with different thickness of amorphous silica shells.

In Ge–silica core–shell hybrid structure, silica layer provides a chemically and mechanically stable medium, which can protect the encapsulated Ge NWs from external disturbance and perturbations and use as a platform for further functionalization. Functionalized silica is a common solid host for embedding fluorescent dyes which have good stability and biocompatibility in biological applications.[52] Furthermore, the silica solid host can take advantage of preventing the self-quenching of dye molecular decreasing the unwanted energy transfer.[53]

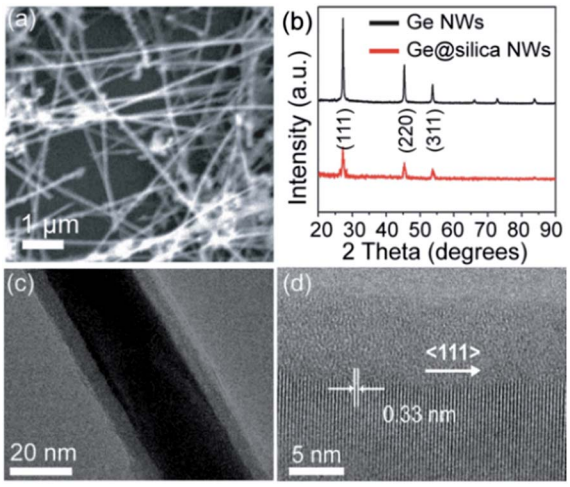

Fig. 5 Characterization of Ge–silica core–shell structure. (a) SEM image. (b) XRD pattern of as-prepared Ge NWs (black line) and Ge–silica core–shell (red line) (c) TEM image and (d) HRTEM image.

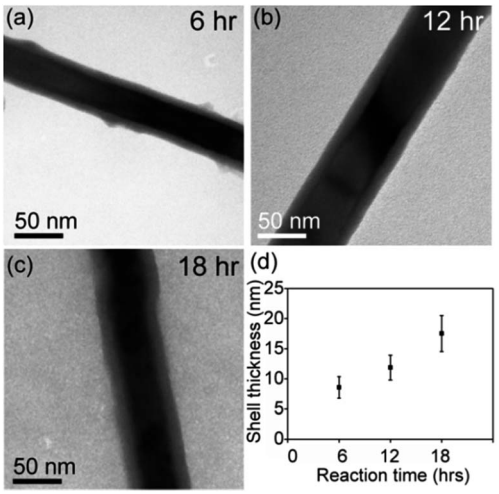

Fig. 7 TEM image of Ge–silica core–shell structure with different reaction time: (a) 6 h, (b) 12 h and (c) 18 h. And the analysis of the silica shell thickness *vs.* reaction time.

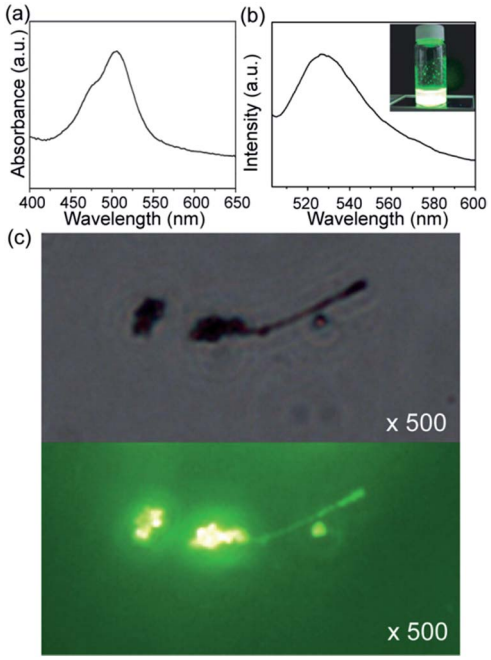

Fig. 8 (a) UV-Vis absorbance spectra and (b) PL spectra of FITC doped Ge–silica core–shell NWs. The inset of (b) is the sample illuminated by UV light. (c) Optical microscope image and fluorescence microscope image of FITC doped Ge–silica core–shell NWs.

We demonstrated that FITC could be incorporated onto silica shell. APTES is one of the most frequently used organosilane coupling agents for conjugation with FITC. APTES was attached onto the Ge–silica surface followed by FITC incorporation. After overnight stirring, FITC was conjugated on the functionalized Ge–silica core–shell structure. The product was characterized by UV, PL and fluorescence microscope. When the sample was illuminated by UV light at the wavelength of 380 nm, it emitted green light. From UV-Vis spectra, the presence of strong peaks around 490 and 512 nm are typical FITC absorption position. Fluorescence excitation and emission spectra for Ge–silica–FITC shows an obvious peak at around 530 nm. Using a fluorescence microscope setup, it's approved that the FITC was successfully incorporated onto the Ge–silica NWs structure, as shown in Fig. 8.

Conclusions

In summary, we applied the Stöber approach to prepare Ge–silica NWs core–shell nanowires. Isoprene-protected Ge NWs were mixed with TEOS and ammonia solution to form a uniform layer of SiO_2. With the monolayer organic passivation, the surface etching of Ge NWs in the aqueous solution can be avoided. The thickness of the silica shell can be varied from 6–20 nm with various reaction time. The silica not only increases the stability, but also allows the Ge NWs incorporated with FITC on the surface. This study gives precise control of the interfaces in 1D heterostructures, which is crucial in the assembly of electronic, biological and optoelectronic devices.

Acknowledgements

The authors acknowledge the financial support by the Ministry of Science and Technology of Taiwan (NSC 102-2221-E-007-023-MY3, NSC 102-2221-E-007-090-MY2, NSC 101-2623-E-007-013-IT, and NSC 102-2633-M-007-002), the Ministry of Economic Affairs, Taiwan (101-EC-17-A-09-S1-198), National Tsing Hua University (102N2051E1), and the assistance from Center for Energy and Environmental Research, National Tsing-Hua University.

Notes and references

1 X. Y. Wu, J. S. Kulkarni, G. Collins, N. Petkov, D. Almecija, J. J. Boland, D. Erts and J. D. Holmes, *Chem. Mater.*, 2008, **20**, 5954–5967.
2 C. O'Regan, S. Biswas, N. Petkov and J. D. Holmes, *J. Mater. Chem. C*, 2014, **2**, 14–33.
3 C. K. Chan, X. F. Zhang and Y. Cui, *Nano Lett.*, 2008, **8**, 307–309.
4 Y. Y. Wu and P. D. Yang, *J. Am. Chem. Soc.*, 2001, **123**, 3165–3166.
5 H. Y. Tuan, D. C. Lee, T. Hanrath and B. A. Korgel, *Chem. Mater.*, 2005, **17**, 5705–5711.
6 B. M. Wen, Y. Z. Huang and J. J. Boland, *J. Mater. Chem.*, 2008, **18**, 2011–2015.
7 H. J. Yang and H. Y. Tuan, *J. Mater. Chem.*, 2012, **22**, 2215–2225.
8 C. Claeys and E. Simoen, *Germanium-based technologies: from materials to devices*, Elsevier, 2011.
9 F. W. Yuan, H. J. Yang and H. Y. Tuan, *ACS Nano*, 2012, **6**, 9932–9942.
10 E. J. Klem, H. Shukla, S. Hinds, D. D. MacNeil, L. Levina and E. H. Sargent, *Appl. Phys. Lett.*, 2008, **92**, 212105.
11 G. I. Koleilat, L. Levina, H. Shukla, S. H. Myrskog, S. Hinds, A. G. Pattantyus-Abraham and E. H. Sargent, *ACS Nano*, 2008, **2**, 833–840.
12 D. V. Talapin and C. B. Murray, *Science*, 2005, **310**, 86–89.
13 J. Tang, K. W. Kemp, S. Hoogland, K. S. Jeong, H. Liu, L. Levina, M. Furukawa, X. Wang, R. Debnath and D. Cha, *Nat. Mater.*, 2011, **10**, 765–771.
14 W.-K. Hong, J. I. Sohn, D.-K. Hwang, S.-S. Kwon, G. Jo, S. Song, S.-M. Kim, H.-J. Ko, S.-J. Park, M. E. Welland and T. Lee, *Nano Lett.*, 2008, **8**, 950–956.
15 X. Wu, J. S. Kulkarni, G. Collins, N. Petkov, D. Almécija, J. J. Boland, D. Erts and J. D. Holmes, *Chem. Mater.*, 2008, **20**, 5954–5967.
16 T. Hanrath and B. A. Korgel, *J. Phys. Chem. B*, 2005, **109**, 5518–5524.
17 V. C. Holmberg and B. A. Korgel, *Chem. Mater.*, 2010, **22**, 3698–3703.
18 A. Guerrero-Martínez, J. Pérez-Juste and L. M. Liz-Marzán, *Adv. Mater.*, 2010, **22**, 1182–1195.
19 M. H. Huang, A. Choudrey and P. D. Yang, *Chem. Commun.*, 2000, 1063–1064.
20 X. M. Meng, J. Q. Hu, Y. Jiang, C. S. Lee and S. T. Lee, *Appl. Phys. Lett.*, 2003, **83**, 2241–2243.

21 X. C. Wu, W. H. Song, B. Zhao, W. D. Huang, M. H. Pu, Y. P. Sun and J. J. Du, *Solid State Commun.*, 2000, **115**, 683–686.
22 G. Z. Ran, L. P. You, L. Dai, Y. L. Liu, Y. Lv, X. S. Chen and G. G. Qin, *Chem. Phys. Lett.*, 2004, **384**, 94–97.
23 H. Wang, X. Zhang, X. Meng, S. Zhou, S. Wu, W. Shi and S. Lee, *Angew. Chem., Int. Ed.*, 2005, **117**, 7094–7097.
24 S. Y. Bae, H. W. Seo, H. C. Choi, D. S. Han and J. Park, *J. Phys. Chem. B*, 2005, **109**, 8496–8502.
25 Y. Cao, Y. Tang, Y. Liu, Z. Liu, L. Luo, Z. He, J. Jie, R. Vellaisamy, W. Zhang and C. Lee, *Nanotechnology*, 2009, **20**, 455702.
26 M. Afzaal and P. O'Brien, *J. Mater. Chem.*, 2006, **16**, 1113–1115.
27 Y. Zhang, K. Suenaga, C. Colliex and S. Iijima, *Science*, 1998, **281**, 973–975.
28 W.-S. Shi, H.-Y. Peng, L. Xu, N. Wang, Y. Tang and S.-T. Lee, *Adv. Mater.*, 2000, **12**, 1927–1930.
29 J. Huang, W. K. Chim, S. Wang, S. Y. Chiam and L. M. Wong, *Nano Lett.*, 2009, **9**, 583–589.
30 J. Q. Hu, X. M. Meng, Y. Jiang, C. S. Lee and S. T. Lee, *Adv. Mater.*, 2003, **15**, 70–73.
31 W. Stöber, A. Fink and E. Bohn, *J. Colloid Interface Sci.*, 1968, **26**, 62–69.
32 C. Graf, D. L. J. Vossen, A. Imhof and A. van Blaaderen, *Langmuir*, 2003, **19**, 6693–6700.
33 S.-H. Wu, C.-Y. Mou and H.-P. Lin, *Chem. Soc. Rev.*, 2013, **42**, 3862–3875.
34 A. L. Rogach, D. Nagesha, J. W. Ostrander, M. Giersig and N. A. Kotov, *Chem. Mater.*, 2000, **12**, 2676–2685.
35 Y. Wang, Z. Tang, X. Liang, L. M. Liz-Marzán and N. A. Kotov, *Nano Lett.*, 2004, **4**, 225–231.
36 L. M. Liz-Marzan, M. Giersig and P. Mulvaney, *Langmuir*, 1996, **12**, 4329–4335.
37 Y. D. Liu, F. F. Fang and H. J. Choi, *Soft Matter*, 2011, **7**, 2782–2789.
38 J. Y. Kim, S. B. Yoon and J. S. Yu, *Chem. Commun.*, 2003, 790–791.
39 Y. J. Wong, L. F. Zhu, W. S. Teo, Y. W. Tan, Y. H. Yang, C. Wang and H. Y. Chen, *J. Am. Chem. Soc.*, 2011, **133**, 11422–11425.
40 J. C. Park, J. U. Bang, J. Lee, C. H. Ko and H. Song, *J. Mater. Chem.*, 2010, **20**, 1239–1246.
41 W. Li and D. Y. Zhao, *Adv. Mater.*, 2013, **25**, 142–149.
42 C. Hui, C. Shen, J. Tian, L. Bao, H. Ding, C. Li, Y. Tian, X. Shi and H.-J. Gao, *Nanoscale*, 2011, **3**, 701–705.
43 C. Mi, J. Zhang, H. Gao, X. Wu, M. Wang, Y. Wu, Y. Di, Z. Xu, C. Mao and S. Xu, *Nanoscale*, 2010, **2**, 1141–1148.
44 M. Son, S. Jeong and D.-J. Jang, *J. Phys. Chem. C*, 2014, **118**, 5961–5967.
45 Y. Imura, S. Hojo, C. Morita and T. Kawai, *Langmuir*, 2014, **30**, 1888–1892.
46 H. Wang, L. Chen, Y. Feng and H. Chen, *Acc. Chem. Res.*, 2013, **46**, 1636–1646.
47 T. Hanrath and B. A. Korgel, *J. Am. Chem. Soc.*, 2004, **126**, 15466–15472.
48 B. Yoo, A. Dodabalapur, D. C. Lee, T. Hanrath and B. A. Korgel, *Appl. Phys. Lett.*, 2007, **90**, 072106.
49 Y. Kobayashi, H. Katakami, E. Mine, D. Nagao, M. Konno and L. M. Liz-Marzan, *J. Colloid Interface Sci.*, 2005, **283**, 392–396.
50 V. K. Lamer and R. H. Dinegar, *J. Am. Chem. Soc.*, 1950, **72**, 4847–4854.
51 Y. Yin, Y. Lu, Y. Sun and Y. Xia, *Nano Lett.*, 2002, **2**, 427–430.
52 A. Burns, H. Ow and U. Wiesner, *Chem. Soc. Rev.*, 2006, **35**, 1028–1042.
53 A. Imhof, M. Megens, J. Engelberts, D. De Lang, R. Sprik and W. Vos, *J. Phys. Chem. B*, 1999, **103**, 1408–1415.